Developing a hydrological model for evaluating the future flood risks in rural areas

Adeyi, Qudus[a] · Ahmad, Mirza Junaid[b] · Adelodun, Bashir[c,d] · Odey, Golden[e] · Akinsoji, Adisa Hammed[f] ·
Salau, Rahmon Abiodun[g] · Choi, Kyung Sook[h]*

[a]Ph.D Combined Degree Student, Department of Agricultural Civil Engineering, Kyungpook National University, Daegu, Korea
[b]Post-doctoral Researcher, Department of Agricultural Civil Engineering, Kyungpook National University, Daegu, Korea
[c]Post-doctoral Researcher, Department of Agricultural Civil Engineering, Kyungpook National University, Daegu, Korea
[d]Lecturer, Department of Agricultural and Biosystems Engineering, University of Ilorin, Ilorin, Nigeria
[e]Ph. D Candidate, Department of Agricultural Civil Engineering, Kyungpook National University, Daegu, Korea
[f]Ph. D Student, Department of Agricultural Civil Engineering, Kyungpook National University, Daegu, Korea
[g]Ph. D Student, Department of Agricultural Civil Engineering, Kyungpook National University, Daegu, Korea
[h]Professor, Department of Agricultural Civil Engineering, Kyungpook National University, Daegu, Korea

Abstract

Climate change is expected to amplify the future flooding risks in rural areas which could have devastating implications for the sustainability of the agricultural sector and food security in South Korea. In this study, spatially disaggregated and statistically bias-corrected outputs from three global circulation models (GCMs) archived in the Coupled Model Intercomparison Project Phases 5 and 6 (CMIP5 and 6) were used to project the future climate by 2100 under medium and extreme scenarios. A hydrological model was developed to simulate the flood phenomena at the Shindae experimental site located in the Chungcheongbuk Province, South Korea. Hourly rainfall, inundation depth, and discharge data collected during the two extreme events that occurred in 2021 and 2022 were used to calibrate and validate the hydrological model. Probability analysis of extreme rainfall data suggested a higher likelihood of intense and unprecedented extreme rainfall events, which would be particularly notable during 2051-2100. Consequently, the flooded area under an inundation depth of >700 mm increased by 13-36%, 54-74%, and 71-90% during 2015-2030, 2031-2050, and 2051-2100, respectively. Severe flooding probability was notably higher under extreme CMIP6 scenarios than under their CMIP5 counterparts.

Keywords: Extreme rainfall, Hydrological model, Climate change, Flood

농촌지역 미래 홍수 위험도 평가를 위한 수문 모델 개발

쿠두스 아데이[a] · 미르자 주네이드 아흐메드[b] · 바실 아델러둔[c,d] · 오데이 골든[e] · 아디사 하메드 아킨소지[f] ·
라흐몬 아비오던 살라우[g] · 최경숙[h]*

[a]경북대학교 농업토목공학과 석박사통합과정, [b]경북대학교 농업토목공학과 박사후연구원, [c]경북대학교 농업토목공학과 박사후연구원,
[d]나이지리아 일로린대학, 농업생물시스템공학과, 전임강사, [e]경북대학교 농업토목공학과 박사수료, [f]경북대학교 농업토목공학과 박사과정,
[g]경북대학교 농업토목공학과 박사과정, [h]경북대학교 농업토목공학과 교수

요 지

미래 기후변화 현상은 농촌지역의 홍수 위험을 증가 시켜 농업의 지속 가능성과 식량 안보를 위협할 것으로 예견된다. 본 연구에서는 미래기후변화를 파악하기 위해 세 개의 GCM을 선정하여 RCP 및 SSP 시나리오 중 중간 및 극한조건을 각각 적용하여 미래 기후변화를 예측하였다. 충북 청주시 신대지구를 대상으로 미래 홍수 위험도를 평가하기 위한 수문 모델을 개발하였으며, 대상지구에서 발생했던 2021~2022년내 강우사상에 대한 시우량, 유출량 측정자료를 사용하여 수문 모델을 검보정 하였다. RCP와 SSP 시나리오에 의한 미래 기상자료를 활용하여 홍수 위험 정도를 비교 분석한 결과. 미래로 갈수록 극한 강우 발생가능성이 높아지는 경향을 보여, 2051~2100년 기간에 극한강우 발생 가능성이 가장 높게 나타났다. 대상지구에서 발생한 침수심이 700 mm를 초과하는 경우는 2015~2030년 기간에는 13~36%, 2031~2050년 기간에는 54~74%, 2051~2100년 기간에는 71~91%를 각각 차지하는 것으로 나타났다. 또한 RCP 시나리오 보다 SSP 시나리오에 적용한 미래 기후변화 조건에서 극한 홍수 발생 가능성이 더 높게 나타나는 것으로 평가되었다.

핵심용어: 극한 강우, 수문 모델, 기후변화 , 홍수

*Corresponding Author. Tel: +82-53-950-5731
E-mail: ks.choi@knu.ac.kr (Choi, Kyung Sook)

1. Introduction

Climate change is aggravating the frequency, intensity, and severity of extreme hydrological events, such as floods, droughts, typhoons, rising sea levels, and heat waves, resulting in increased risks and damage to lives and properties (Qin and Lu, 2014; Zhang *et al.*, 2019). Furthermore, these events are significantly impacting sustainable global food production, water resources availability and management, biodiversity loss, and population exposure to heat waves (Calvin *et al.*, 2023). Among the extreme events, floods are one of the most severe natural disasters, with approximately 2.2 billion people at risk of damage and loss during 1-in-100-year flood events (Rentschler and Salhab, 2020). Between 1970 and 2021, the floods claimed two million lives and caused economic losses of up to 4.3 trillion US dollars (WMO, 2023). Therefore, it is crucial to assess the impacts of climate change on the occurrence probability of floods to ensure economic, social, and environmental sustainability.

South Korea is among the countries most susceptible to climate change due to its tropical monsoon climate. In recent years, extreme rainfall patterns caused by climate change have been observed nationwide (Adelodun *et al.*, 2023). In July 2023, South Korea experienced the third-highest recorded rainfall event and heaviest rainfall in 150 years, demolishing 9,200 homes and displacing over 14,400 people. This event also damaged over 34,000 hectares (ha) of farmland and caused the death of more than 825,000 livestock nationwide (Chang, 2023). Managing and preventing future floods will be a daunting task, as the country receives up to 60% of the annual rainfall from July to September, often resulting in riverine, flash, and urban floods (Moazzam *et al.*, 2022).

Several studies have investigated the impacts of climate change on flooding at global, national, regional, and catchment scales (Eccles *et al.*, 2021; Han *et al.*, 2022; Hosseinzadehtalaei *et al.*, 2021; Xu *et al.*, 2023; Zhang *et al.*, 2019). Most of these studies combine bias-corrected climate change projections from global climate models (GCMs) or regional climate models (RCMs) and hydrological models, such as SWAT, HEC-HMS, TOPMODEL, FLO-2D, MIKESHE, SWMM, and HEC-RAS to simulate the behaviors of the

physical processes of flooding (Goldenson *et al.*, 2023; Kim *et al.*, 2020; Xu *et al.*, 2005).

Son *et al.* (2010) utilized future climate change data from 13 GCMs to examine the probability of extreme rainfall, associated flood volume, and flood level of the Namhangang River in South Korea. The authors reported that climate change led to 13.0-15%, 29-33.5%, and 12.6-13.6% increase in the occurrence probability of extreme rainfall, flood volume, and flood level. Hwang *et al.* (2018) investigated the influences of climate change on design flood levels in the Hwajabae drainage basin, Seoul, South Korea, using XP-SWMM. The study concluded that the peak flood volume would increase in the future and stressed the need to redesign urban drainage facilities to accommodate extreme flooding. Kwak *et al.* (2020) evaluated the effects of climate change scenarios (RCP4.5/8.5 and SSP 2-45/5-85), rainfall distribution, and curve number (CN) on changes in flood volume in the Yedang watershed using HEC-HMS simulations. Although previous studies provide valuable findings and suggestions for adaptive management of future floods, these were mostly focused on urban flooding. Despite the importance of agriculture to the country's economic development, environmental sustainability, and food security, little attention has been paid to understanding the impact of the changing climate on flooding in agricultural watersheds in South Korea (Kim *et al.*, 2018; Lee and Shin, 2021).

In South Korea, flooding greatly affects agricultural areas, leading to critical consequences, including crop damage, soil degradation, and loss of arable lands (Li *et al.*, 2021). Therefore, the primary purpose of this study was to estimate the impact of future climate on flood risks in agricultural areas in South Korea. To achieve this aim, we evaluated and compared the occurrence probability of extreme rainfall events based on the long-term historical and future climate change data. A hydrological model was developed to simulate the flooding phenomenon in rural areas based on the hourly recorded rainfall, discharge, and inundation depth data collected from the Shindae experimental site. Finally, the inundation depth of future floods under medium and extreme scenarios was assessed. The study results help gain insight into the flood risks under climate change conditions for the Shindae experimental site, and the developed hydrological

model can be applied to other agricultural regions in South Korea.

2. Methodology

2.1 Study area

In South Korea, the Chungcheongbuk Province is one of the main agricultural-producing provinces which has been frequently experiencing heavy rainfalls, floods, and droughts due to climate change (Adelodun *et al*., 2022). We selected the Shindae experimental site in Chungcheongbuk Province, because of the availability of relevant data and information required to simulate flood phenomena in an agricultural area. The size of the study area was 4.8 km^2, and it is located between 36.660^o N-36.680^o N and 127.400^o E-127.450^o E with elevation ranging between 28.1 and 36.56 m (Fig. 1).

The primary land-use types in the study area are paddy fields, upland crop fields, fruit orchards, and greenhouses, accounting for 87.93% (4.22 km^2), 3.29% (0.16 km^2), 0.08% (0.004 km^2), and 8.70% (0.42 km^2) of the total area, respectively. The study area has also been part of a drainage improve-

ment project managed by the Korea Rural Community Corporation. The mean annual rainfall and temperature measured between 1974 and 2020 are 1219 mm and 12.5^{o}C, respectively (Adelodun *et al*., 2022). The drainage system in the study area drains into the Seoknamcheon Stream and flows into the Geumgang River.

2.2 Datasets

Spatial data used in this study include the 20 cm resolution DEM acquired from the National Geographic Information Institute, a farm map of the study site created by the Ministry of Agriculture, Food and Rural Affairs, actual survey data, and drainage structure specifications. We used historical rainfall data (1975-2014) from Cheongju weather station to calculate the occurrence probability of extreme rainfall events. Furthermore, hourly rainfall, inundation depth, and discharge data were collected in the field during the summers of 2021-2023 (June-August).

Future climate change projections were derived from three Coupled Model Intercomparison Project 5 and 6 (CMIP5 and CMIP6) GCMs (Table 1), which have been reported to be the best-performing GCMs for simulating the seasonal, annual
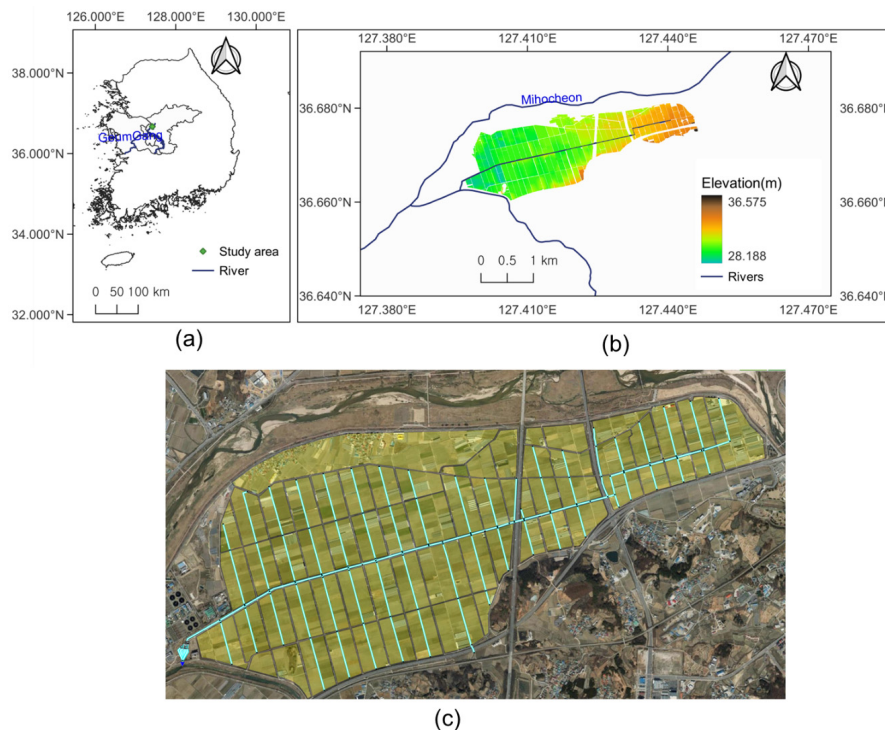

Fig. 1. (a) Location of the study area, (b) Elevation profile of the study area, (c) picture of the study area

Table 1. Names and Institute of selected GCMs

Modelling Center	CMIP5	CMIP6
Commonwealth Scientific and Industrial Research Organization and Bureau of Meteorology, Australia	ACCESS1-3	-
Beijing Climate Center, China Meteorological Administration, China	-	BCC-CSM2-MR
NOAA Geophysical Fluid Dynamics Laboratory, USA	-	GFDL-ESM4
NASA Goddard Institute Space Studies	GISS-E2-R	
Meteorological Research Institute, Japan	MRI-CGCM3	MRI-ESM2-0

climate change patterns in this area (Ahmad and Choi, 2023; Park *et al.*, 2021; Song *et al.*, 2021; Adelodun *et al.*, 2023). Daily GCMs outputs forced under two representative concentration pathway (RCP) scenarios: RCP4.5 and RCP8.5, and two shared socioeconomic pathway (SSP) scenarios: SSP2-4.5 and SSP5-8.5, were used to project future rainfall during three time slices: S1 (2015-2030), S2 (2031-2050), and S3 (2051-2100). The future rainfall data were downscaled and bias-corrected following the procedure previously reported in another study (Ahmad and Choi, 2023). Multi-model ensembles of the GCMs under different climate change scenarios were used to account for the uncertainties and variations in the individual models and thereby improve the reliability and accuracy of the climate change projection (Karmalkar *et al.*, 2019; Tegegne *et al.*, 2020).

2.3 Frequency analysis of rainfall data

Frequency analysis is an essential tool to understand the probability of extreme rainfall events, which is crucial for various applications such as designing hydraulic structures and analyzing erosion and flood problems. Different probability distributions, such as log-normal, Gumbel, log-Pearson type III, and normal frequency distributions, have been used to analyze the occurrence probability of extreme rainfalls and floods. These analyses are based on statistical methods and involve fitting probability distributions to recorded rainfall data (Badou *et al.*, 2021; Al-Awadi *et al.*, 2023).

In this study, the annual maximum daily precipitation data in the baseline (1975-2014) and future time slices (S1-S3) were extracted and fitted to the Gumbel distribution (Eqs. (1) and (2)) using the probability-weighted moment as the parameter estimation method. Gumbel distribution has been identified as the optimal probability distribution type of point frequency rainfall in South Korea (MLTM, 2012; ME, 2019).

$$PDF : f(x) = \frac{1}{\beta} exp\left(-\frac{x-\mu}{\beta} - e^{\frac{x-\mu}{\beta}}\right) \tag{1}$$

$$CDP : F(x) = \exp\left(-e^{-\frac{x-\mu}{\beta}}\right) \tag{2}$$

where x is the random variable, μ is the location parameter, and β is the scale parameter.

2.4 Hydrological modelling

A hydrological model was developed in this study to simulate the flood phenomenon at the study site. The simulation process included the construction of a drainage system network, hydrological calculation of the flood volume in each sub-block, and calculation of the design volume at the final drain through flood tracking and synthesis.

2.4.1 Development of flood simulation model

The drainage system of the study area was imported into the hydrological model as a network of nodes (junction points) and links (channels) along with the elevation and spatial location of the drainage system elements. The drainage system network comprised 137 nodes and 129 links, and the entire area was divided into 63 drainage blocks, each centered on a drainage channel (Fig. 2). Flow dynamics in the drainage system were simulated using the St. Venant's one-dimensional unsteady flow equations as follows:

$$\frac{\partial A}{\partial t} + \frac{\partial Q}{\partial x} = 0 \tag{3}$$

$$\frac{\partial Q}{\partial t} + \frac{\partial}{\partial x}\left(\frac{Q^2}{A}\right) + gA\frac{\partial H}{\partial x} + gAS_{f=0} \tag{4}$$

where Q is runoff (m^3/s), S_f is the slope of a sub-block, and

Fig. 2. Drainage network at the study site comprising nodes, links, and drainage blocks

A is the cross-sectional area of surface flow in a sub-block (m^2). Eqs. (3) and (4) were implemented using the extended transport (EXTRAN) block in the Storm Water Management Model (SWMM).

2.4.2 Flood volume calculation

The flood volume was calculated based on rainfall-runoff theory and unit hydrograph. This study employed the soil conservation service (SCS) dimensionless unit diagram method. Type III standard curve number index (CN III) was selected to represent the flood-causing direct runoff generation in the watershed when the soil remains saturated or nearly saturated with limited infiltration capacity. This mimics worst-case scenarios that can be encountered on the field. The rainfall-runoff theory was applied to calculate the effective rainfall that contributes to direct runoff, excluding losses from actual rainfall. In each sub-block, runoff generated because of the effective rainfall was estimated using the unit hydrograph. The duration of the effective rainfall (D) was estimated as a function of the total rainfall time (t_r) using Eq. (5). The peak occurrence time (t_p) and peak flow rate (q_p) were derived using Eqs. (8) and (9). The rainfall was then redistributed by duration around t_p. The longitudinal axes (q_1, q_2, $\cdots$ q_n) of the unit diagram corresponding to the duration were calculated using the relationship between t/t_p and q/q_p (Al-Ghobari *et al.*, 2020; Im and Park, 1997; Tramblay *et al.*, 2010).

$$S = \frac{25,000}{CN} - 254 \tag{5}$$

$$Q = \frac{(P - 0.2S)^2}{P + 0.8S} \tag{6}$$

$$D = 0.133t_r \tag{7}$$

$$t_p = \frac{D}{2} + 0.6t_r \tag{8}$$

$$q_p = \frac{0.208AQ}{t_p} \tag{9}$$

where A is the area in km^2, Q is the runoff depth (mm), and S is the potential maximum soil moisture retention after the runoff begins (mm). The Muskingum flood routing method was applied to estimate the temporal change in flooding from upstream to downstream (Kim *et al.*, 2023; Mohammad, 1978).

2.5 Model calibration and validation

The hydrological model was calibrated to understand and minimize the difference between the simulated and measured discharges in the study area. Hourly data of inundation depth, discharge, and rainfall collected during the storm event on August 23-25, 2021, were used to calibrate the time of concentration (t_c) and CN. Based on the calibrated parameters, the simulated discharge data were compared with the discharge data collected between August 10-15, 2022, to validate the hydrological model. The Nash-Sutcliffe efficiency (NSE), root mean square error (RMSE), and Kling-Gupta efficiency (KGE) were used to evaluate the model performance and error metrics, as shown in Eqs. (10)~(12):

$$NSE = 1 - \frac{\sum_{i=1}^{n}(Q_{obs,i} - Q_{sim,i})^2}{\sum_{i=1}^{n}(Q_{obs,i} - \overline{Q}_{obs})^2} \tag{10}$$

$$RMSE = \sqrt{\frac{1}{n}\sum_{i=1}^{n}(Q_{obs\,i} - Q_{sim\,i})^2} \tag{11}$$

$$KGE = 1 - \sqrt{(r-1)^2 + (\beta-1)^2 + (a-1)^2} \tag{12}$$

where Q_{obs} and Q_{sim} are observed and simulated discharge values at each time-step, n is the total number of observations or total time steps, $\overline{Q}_{obs}$ is the mean of the observed discharge, r is the Pearson correlation coefficient, β is the ratio of the standard deviation of simulated discharge to that of observed discharge, and a is the ratio of the means of simulated to means of observed discharges.

3. Results & Discussions

3.1 Rainfall distribution pattern

Annual maximum daily rainfall data during the baseline and future time slices were compared to comprehend the occurrence probability of heavy rainfall events. During the baseline period, the average annual daily maximum rainfall was 131 mm. Under RCP8.5, SSP2-4.5, and SSP5-8.5, the average annual maximum daily rainfall was projected to decrease in the S1 period and increase under RCP4.5. Furthermore, the average annual maximum daily rainfall was projected to increase across all climate change scenarios in the S2 and S3 periods, with a more notable increase in the S3 period compared to other periods. Overall, these results indicate an anticipated increase of 8-23% in average annual maximum daily rainfall in the future (S2 and S3 periods), with an average reduction of 3-9% in the S1 period.

To understand the occurrence probability of extreme rainfall events under climate change scenarios, we fitted a Gumbel probability distribution to the annual maximum daily rainfall data using the probability-weighted moment method for parameter estimation. Fig. 3 shows the probability density functions of the fitted rainfall data during the baseline and future periods. The frequency of extreme events is more dependent on variance (scale parameter) compared to the mean (location parameters) (Katz and Brown, 1992). Therefore, assessing these variations is crucial for interpreting the impact of climate change on extreme events.

Under the RCP4.5 scenario, notable shifts in the location and scale parameters suggest frequent extreme rainfalls and the shifts were notably evident during S3 (Fig. 3(a)). In contrast, under RCP8.5 and SSP2-4.5, projections indicate an increase in the scale parameter along with a reduction in the location parameter for all the future periods except the S1 period, indicating high variability in the future rainfall distribution under RCP8.5 and SSP2-4.5 (Figs. 3(b) and 3(c)). Under the SSP5-8.5, the pattern of climate variability in the S1 period aligns with the baseline, whereas the variance and mean increase in the S2 and S3 periods (Fig. 3(d)). Overall, our results show a higher frequency of future rainfall events with
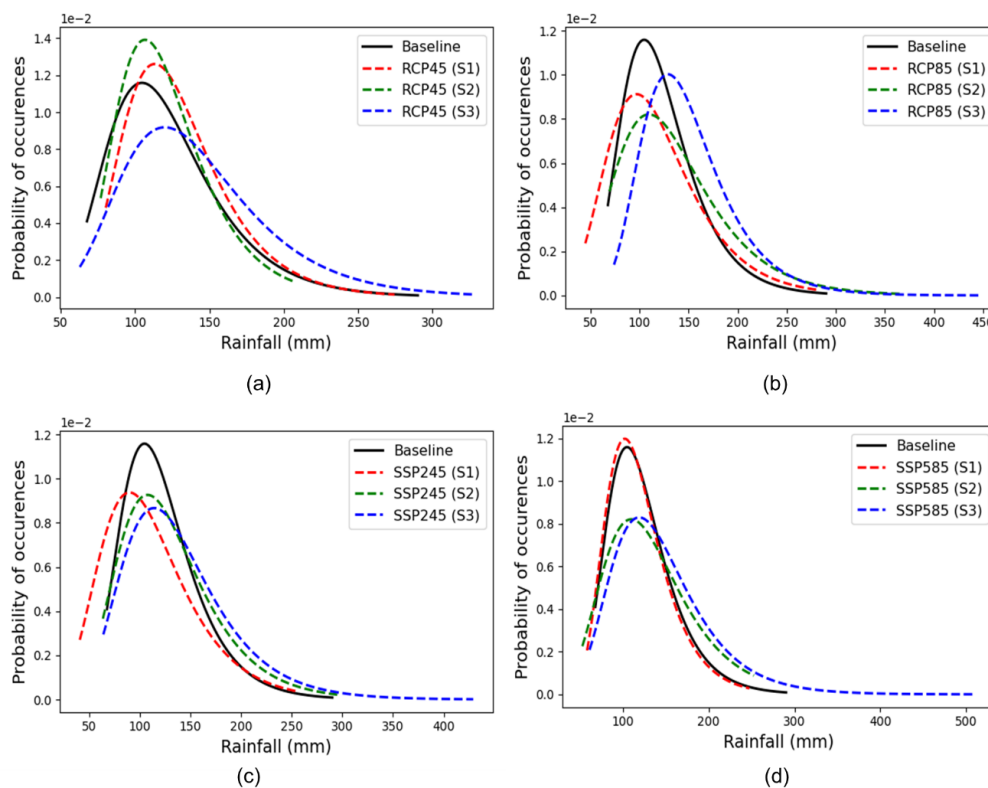

(a)   (b)

(c)   (d)

Fig. 3. Probability distribution of rainfall during baseline and future time slices under (a) RCP45, (b) RCP85, (c) SSP2-4.5 and (d)SSP5-8.5 scenarios

higher uncertainty.

3.2 Calibration and validation of the hydrological model

This study focused on estimating two critical parameters, t_c and CN, essential for calibrating the hydrological models (de Almeida *et al*., 2016; Hawkins *et al*., 2019). Peak discharge rate and flood event timing are highly dependent on the key catchment response time parameter (t_c) (Kousari *et al*., 2010). Its estimation relies on variables from monitoring rainfall-runoff events in a watershed (Perdikaris *et al*., 2018). The SCS curve number method is commonly used to estimate peak discharge in watersheds (Garg *et al*., 2003). CN significantly influenced the peak discharge estimation, and its sensitivity increased with the return period of rainfall. Therefore, a precise estimate of t_c and CN is crucial for calibrating hydrological models and improving the accuracy of hydrological simulations.

The hydrological model was calibrated using field-measured rainfall and discharge data from August 23 to 25, 2021. Fig. 4(a) shows the comparison between the simulated and measured discharges during calibration. The hydrological model simulated slightly mismatched discharge during the calibration and validation periods which could be attributed to the model's assumptions: uniform land cover, CN, and soil characteristics. Under actual field conditions, these parameters could be spatially heterogeneous. However, the observed and simulated discharges were sufficiently corroborated (Althoff and Rodrigues, 2021). After calibration, the model showed satisfactory performance in simulating the

measured discharge with the NSE, KGE, and RMSE values of 0.75, 0.70, and 0.53 m^3s^{-1}, respectively (Fig. 4). During the validation phase, the model performance was slightly reduced, but the NSE, KGE, and RMSE values remained within acceptable limits (Fig. 4(b)). Overall, the model satisfactorily simulated the flooding phenomena in the study area, indicating its reliability for predicting future floods.

3.3 Inundation under climate change scenarios

The hydrological model was applied to simulate inundation in the study area using extreme rainfall during the baseline and future time slices. We used three inundation depths to explain the magnitude of flooding: inundation depths of < 300 mm, 300-700 mm, and > 700 mm representing normal, moderate, and extreme flooding, respectively. The relative changes in the area under inundation considering climate change scenarios were also computed for the future period with respect to the baseline. Fig. 5 shows the area under normal, moderate, and extreme inundation depths during the baseline and future time slices.

During the baseline period, out of 4.80 km^2, 3.57 km^2 (74%) remained under normal, while 0.41 km^2(9%) and 0.83 km^2(17%) were in moderate and extreme inundation, respectively. All the climate change scenarios projected that the area under extreme inundation would increase in the future, particularly under the SSP 5-8.5 scenario and during the S2 and S3 periods. During the S1, the moderate flooded area increased by 5-21 % regardless of the scenarios, except under RCP 4.5, where it decreased by 0.38%. During the S2
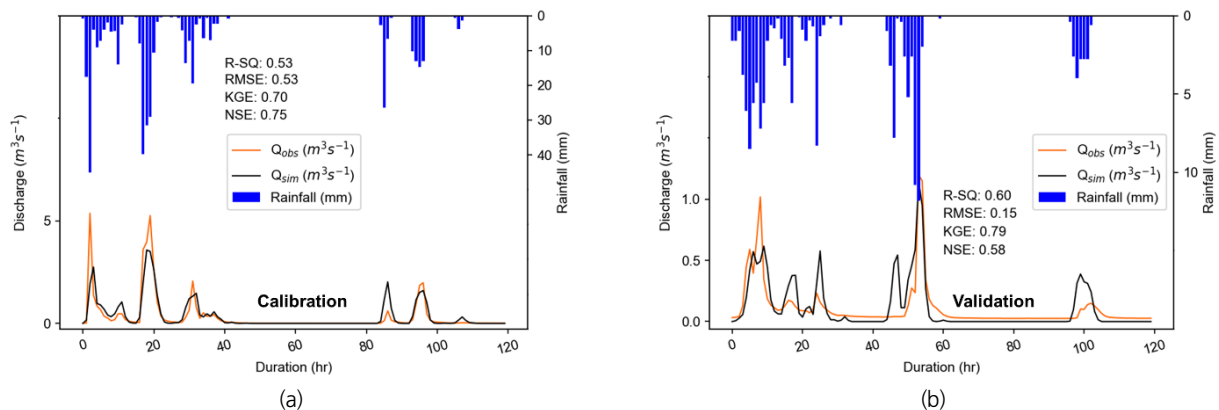

Fig. 4. Performance evaluation of the hydrological model during (a) calibration and (b) validation periods based on Nash-Sutcliffe efficiency (NSE), root mean square error (RMSE), and Kling-Gupta efficiency (KGE)

and S3, the moderately flooded area was projected to decline under all emission scenarios, except under RCP4.5, when moderately flooded areas increased by 9.80% and 8.64%, while the flooded area with extreme inundation depth was projected to increase by 51.50-74%.

A significant percentage of the study area was heavily inundated because of frequent intense rainfall, regardless of the emission scenarios. These findings are consistent with the
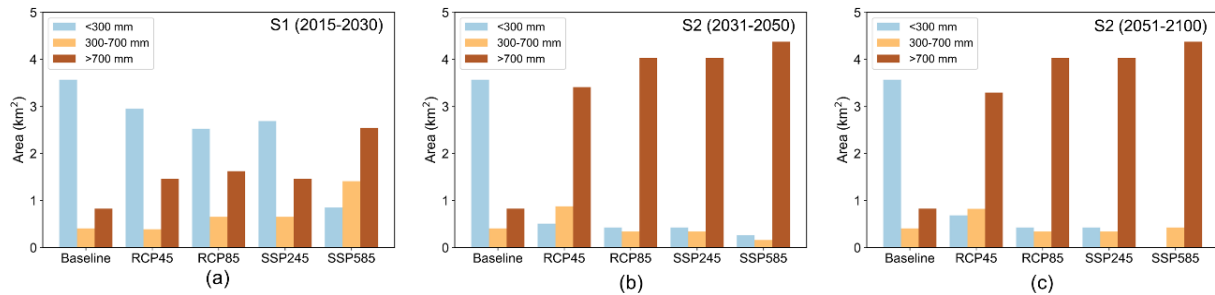

Fig. 5. Area under various inundation depths considering baseline and climate change scenarios during (a) S1(2015-2030) (b) S2 (2031-2050) and (c) S3 (2051-2100)
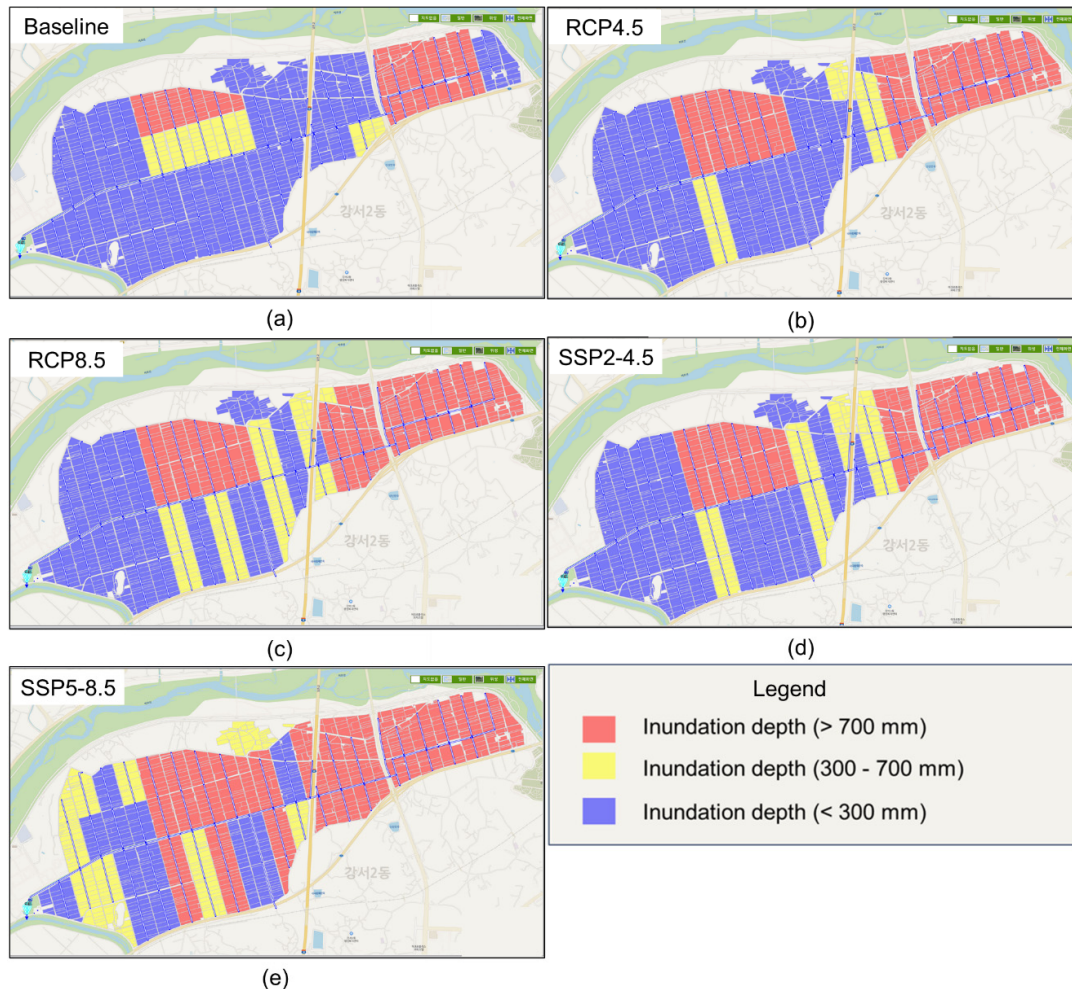

Fig. 6. Spatial distribution of inundation during the baseline and S1 period (2015-2030) under (a) baseline, (b) RCP4.5, (c) RCP8.5, (d) SSP2-4.5 and (e) SSP5-8.5 scenario. Blue represents inundation depth < 300 mm, yellow represents inundation depth between 300 and 700 mm, and red represents inundation depth > 700 mm

results obtained by Edamo *et al*. (2023) in a study conducted in Ethiopia, where he projected that flooding would increase in the future under climate change with an extreme flood in the 2050s under RCP8.5 climate scenarios (Edamo *et al*., 2023). Similarly, in another study conducted in China and Indonesia, flooded areas with higher inundation depths (exceeding 0.5 m) were projected to increase under climate change scenarios (Li *et al*., 2021; Zhang *et al*., 2019).

The projection of changes in inundation depth under a changing climate is essential for developing and implementing informed adaptation strategies. To identify the parts of the study area that are more vulnerable to flooding, we examined the spatial variation of the flood extent during the baseline and future scenarios, and the results are shown in Figs. 6~8.

During baseline, 73% (46 drainage blocks) of the study area were under normal inundation, while 3% (2) and 24% (15) were under moderate and extreme inundation, respectively, with all the drainage blocks under extreme inundation located at the northwestern and northeastern part of the field (Fig. 6(a)). During S1, the number of drainage blocks under normal inundation reduced within 13(21%) and 32(51%) and those with moderate inundation increased to 6(10%)-12(19%) and leaving 23-39 drainage blocks under extreme inundation (Figs. 6(b)~6(e)). The drainage blocks with extreme inundation are in the upstream of the study area; this could be attributed to its nearly flat slope and narrower channels.

The number of drainage blocks with extreme inundation increased to 43(68%) - 59(94%) during the S2 and S3 periods
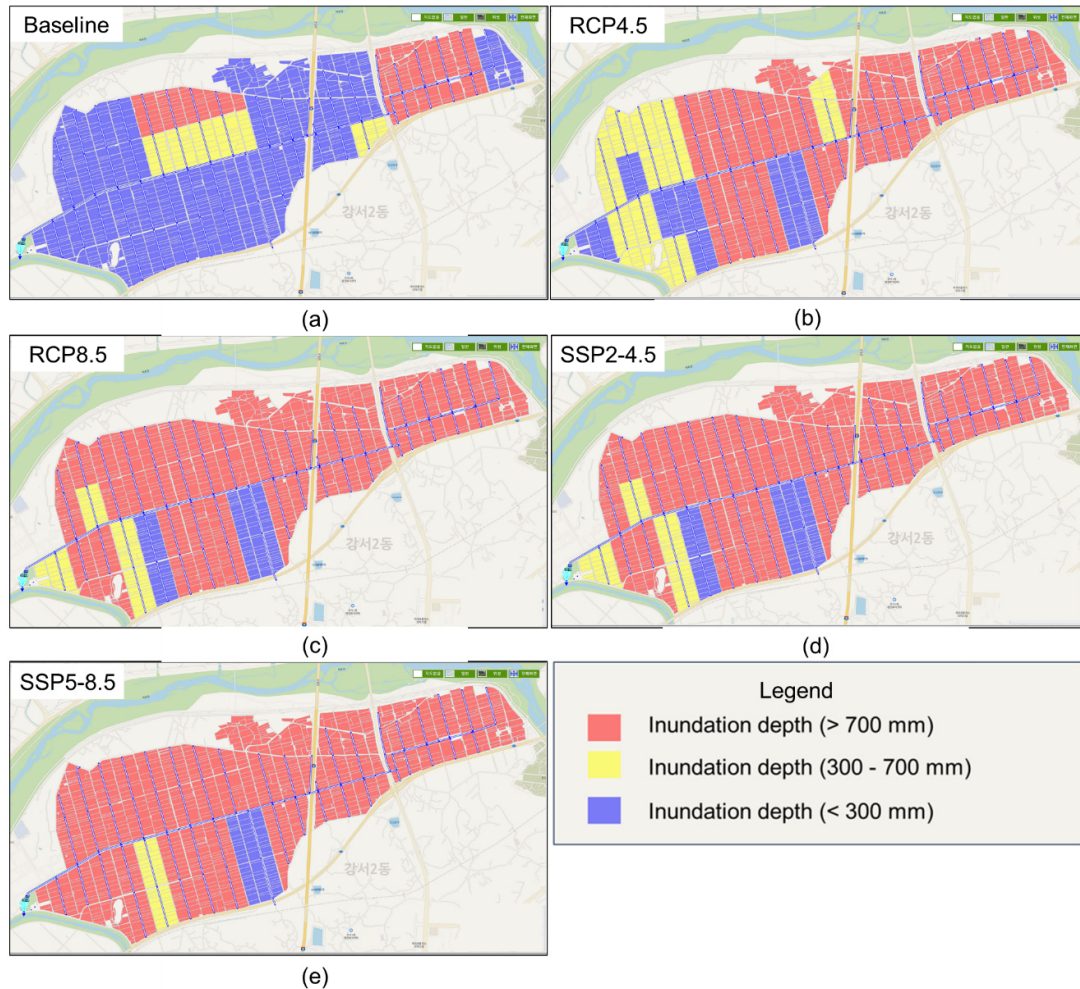

Fig. 7. Spatial distribution of inundation during the baseline and S2 period (2031-2050) under (a) baseline, (b) RCP4.5, (c) RCP8.5, (d) SSP2-4.5 and (e) SSP5-8.5 scenario. Blue represents inundation depth ＜ 300 mm, yellow represents inundation depth between 300 and 700 mm, and red represents inundation depth ＞ 700 mm
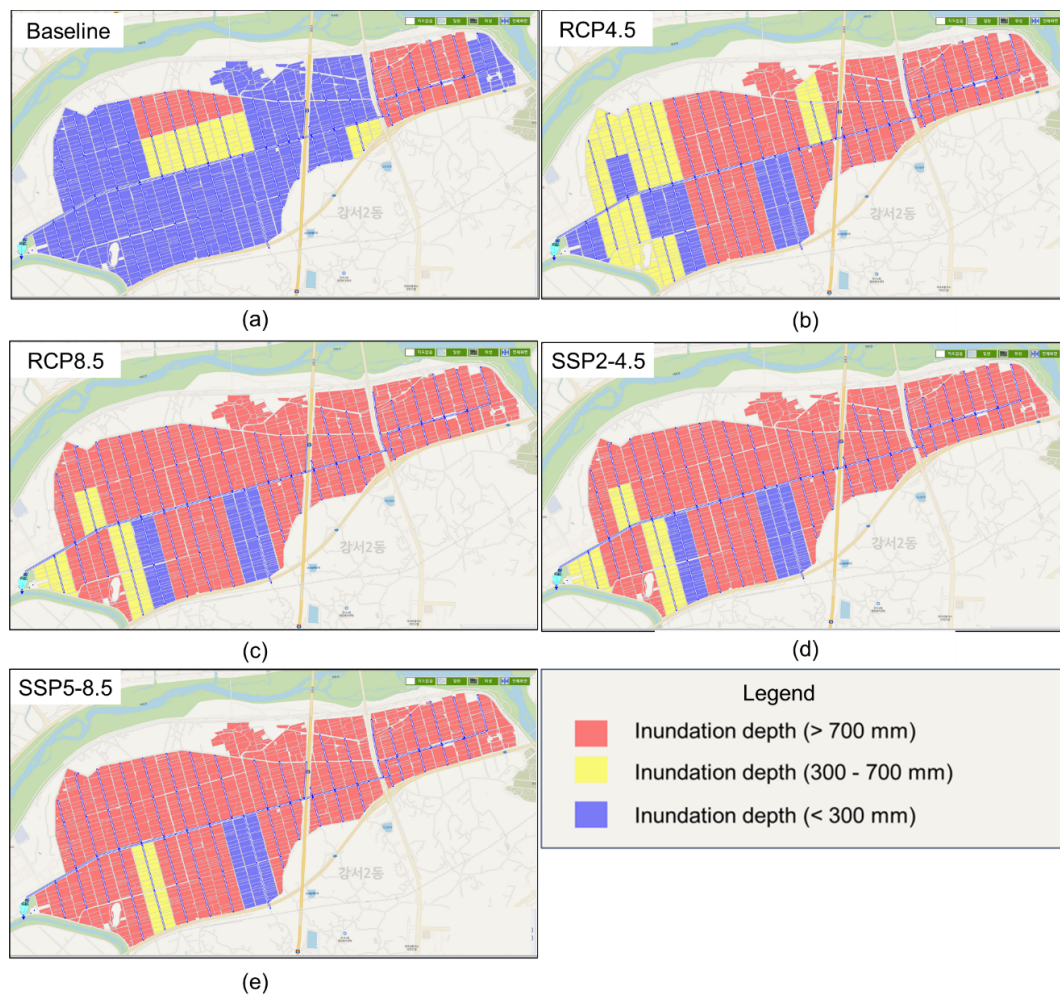
Fig. 8. Spatial distribution of inundation during the baseline and S3 period (2051-2100) under (a) baseline, (b) RCP4.5, (c) RCP8.5, (d) SSP2-4.5 and (e) SSP5-8.5 scenario. Blue represents inundation depth < 300 mm, yellow represents inundation depth between 300 and 700 mm, and red represents inundation depth > 700 mm

with more extreme inundation conditions during S3 period while the drainage blocks with moderate inundation reduced to 2-13 and drainage blocks with normal inundation reduced to 2-7 drainage blocks (Figs. 7 and 8). These results show that under extreme rainfall, the upstream of the study will be inundated than the downstream.

4. Conclusions

The study highlights the importance of understanding and projecting future flood risks, especially in rural areas of South Korea. Climate change impacts on the occurrence probability of future floods were simulated by using the field data

collected at the Shindae experimental site, Chungcheongbuk Province, South Korea. The assessment of the future climate pattern revealed an anticipated increase in extreme rainfall events in the study area. The probability distribution function curve showed a higher shift in variance than that of the mean, which further suggested that the severity of future extreme rainfall events would progressively become more unpredictable. The hydrological model developed in this study showed good performance in simulating the flood processes. Hence, the model can be applied to other locations provided the t_c, CN, and other required site information are available. During 2015-2050, most floods could be categorized as moderate, featuring an inundation depth of 300-700 mm, whereas, during 2051-2100, a typical flood would have an

inundation depth of greater than 700 mm. Upstreams of the study area were highly susceptible to flooding due to narrower drainage channels and nearly flat slopes. Hence, the capacity of the drainage system should be reviewed/improved to accommodate such severe future flooding. In this study, a semi-distributed hydrological model was employed, which did not account for the spatial variability of soil characteristics, land use, and climate. Moreover, the GCMs also produce highly uncertain climate projections because of simplified physics and a lack of complete understanding of intricate land-climate interactions. These limitations and uncertainties were not addressed in this study but should be an integral part of future studies. The occurrence probability of future floods was examined based only on the anticipated future rainfall variability. However, the flood phenomenon is also highly dependent on land use variations. Hence, incorporating both the climate and land use variations when gauging the future flood risks could be more conclusive for devising mitigation plans. Despite acknowledging limited data availability and multiple sources of uncertainties, the study outcomes could be instrumental in managing future flood risks. The strategies to improve flooding resilience must be given priority. These could include the reconstruction of infrastructure, implementation of land use management practices, and development of early warning systems.

Acknowledgement

Conflicts of Interest

The authors declare no conflict of interest.

References

Adelodun, B., Ahmad, M.J., Odey, G., Adeyi, Q., and Choi, K.S. (2023). "Performance-Based evaluation of CMIP5 and CMIP6 global climate models and their multi-model ensembles to simulate and project seasonal and annual climate variables in the Chungcheong region of South Korea." *Atmosphere*, MDPI, Vol. 14, No. 10, pp. 1569-1595.

Adelodun, B., Odey, G., Cho, H., Lee, S., Adeyemi, K.A., and Choi, K.S. (2022). "Spatial-temporal variability of climate indices in Chungcheong provinces of Korea: Application of graphical innovative methods for trend analysis." *Atmospheric Research*, Elsevier, Vol. 280, 106420.

Ahmad, M.J., and Choi, K.S. (2023). "Spatial-temporal evolution and projection of climate extremes in South Korea based on multi-GCM ensemble data." *Atmospheric Research*, Elsevier, Vol. 289, 106772.

Al-Awadi, A.T., Al-Saadi, R.J.M., and Mutasher, A.K.A. (2023). "Frequency analysis of rainfall events in Karbala city, Iraq, by creating a proposed formula with eight probability distribution theories." *Smart Science*, Vol. 11, No. 3, pp. 639-648.

Al-Ghobari, H., Dewidar, A., and Alataway, A. (2020). "Estimation of surface water runoff for a semi-arid area using RS and GIS-based SCS-CN method." *Water*, MDPI, Vol. 12, No. 7, 1924.

Althoff, D., and Rodrigues, L.N. (2021). "Goodness-of-fit criteria for hydrological models: Model calibration and performance assessment." *Journal of Hydrology*, Elsevier Vol. 600, 126674.

Badou, D.F., Adango, A., Hounkpè, J., Bossa, A., Yira, Y., Biao, E.I., Adounkpè, J., Alamou, E., Sintondji, L.O.C., and Afouda, A.A. (2021). "Heavy rainfall frequency analysis in the Benin section of the Niger and Volta Rivers basins: Is the Gumbel's distribution a one-size-fits-all model?." *Proceedings of the International Association of Hydrological Sciences*, Copernicus, Vol. 384, pp. 187-194.

Calvin, K., Dasgupta, D., Krinner, G., Mukherji, A., Thorne, P.W., Trisos, C., Romero, J., Aldunce, P., Barrett, K., Blanco, G., *et al*. (2023). "IPCC, 2023: Climate change 2023: Synthesis report." *Contribution of working groups I, II and III to the sixth assessment report of the Intergovernmental panel on climate change* Edited by Core Writing Team, Lee, H., and Romero, J., Intergovernmental Panel on Climate Change, Geneva, Switzerland.

Chang, D. (2023). Over 8,000 public, private properties reported damaged from torrential rains, Yonhap News Agency, Accessed November 28 2023, <https://en.yna.co.kr/view/AEN20230722002300325>.

de Almeida, I.K., Almeida, A.K., Steffen, J.L., and Alves Sobrinho, T. (2016). "Model for estimating the time of concentration in watersheds." *Water Resources Management*, Springer, Vol. 30, No. 12, pp. 4083-4096.

Eccles, R., Zhang, H., Hamilton, D., Trancoso, R., and Syktus, J.

(2021). "Impacts of climate change on streamflow and flood-plain inundation in a coastal subtropical catchment." *Advances in Water Resources*, Vol. 147, 103825.

Edamo, M.L., Hatiye, S.D., Minda, T.T., and Ukumo, T.Y. (2023). "Flood inundation and risk mapping under climate change scenarios in the lower Bilate catchment, Ethiopia." *Natural Hazards*, Springer, Vol. 118, No. 3, pp. 2199-2226.

Garg, V., Chaubey, I., and Haggard, B.E. (2003). "Impact of calibration watershed on runoff model accuracy." *Transactions of the ASAE*, ASABE, Vol. 46, No. 5, pp. 1347-1353.

Goldenson, N., Leung, L.R., Mearns, L.O., Pierce, D.W., Reed, K.A., Simpson, I.R., Ullrich, P., Krantz, W., Hall, A., Jones, A., and Rahimi, S. (2023). "Use-inspired, process-oriented GCM Selection: Prioritizing models for regional dynamical downscaling." *Bulletin of the American Meteorological Society*, AMS, Vol. 104, No. 9, pp. E1619-E1629.

Han, H., Kim, D., and Kim, H.S. (2022). "Inundation analysis of coastal urban area under climate change scenarios." *Water*, MDPI, Vol. 14, No. 7, pp. 1159-1178.

Hawkins, R.H., Theurer, F.D., and Rezaeianzadeh, M. (2019). "Understanding the basis of the curve number method for watershed models and TMDLs." *Journal of Hydrologic Engineering*, ASCE, Vol. 24, No. 7, 06019003.

Hosseinzadehtalaei, P., Ishadi, N.K., Tabari, H., and Willems, P. (2021). "Climate change impact assessment on pluvial flooding using a distribution-based bias correction of regional climate model simulations." *Journal of Hydrology*, Vol. 598, 126239.

Hwang, J., Ahn, J., Jeong, C., and Heo, J.-H. (2018). "A study on the variation of design flood due to climate change in the ungauged urban catchment." *Journal of Korea Water Resources Association*, Vol. 51, No. 5, pp. 395-404.

Im, S.-J., and Park, S.-U. (1997). "Estimating runoff curve numbers for paddy fields." *Journal of Korea Water Resources Association*, KWRA, Vol. 30, No. 4, pp. 379-387.

Karmalkar, A.V., Thibeault, J.M., Bryan, A.M., and Seth, A. (2019). "Identifying credible and diverse GCMs for regional climate change studies - case study: Northeastern United States." *Climatic Change*, Springer, Vol. 154, No. 3-4, pp. 367-386.

Katz, R.W., and Brown, B.G. (1992). "Extreme events in a changing climate: Variability is more important than averages." *Climatic Change*, Vol. 21, No. 3, pp. 289-302.

Kim, S., Kwon, J.H., Om, J.S., Lee, T., Kim, G., Kim, H., and Heo, J.H. (2023). "Increasing extreme flood risk under future climate change scenarios in South Korea." *Weather and Climate Extremes*, Elsevier, Vol. 39, 100552.

Kim, S.-M., Kang, M.-S., and Jang, M.-W. (2018). "Assessment of agricultural drought vulnerability to climate change at a municipal level in South Korea." *Paddy and Water Environment*, Springer, Vol. 16, No. 4, pp. 699-714.

Kim, Y., Yu, J., Lee, K., Sung, H.C., and Jeon, S.W. (2020). "Application of the HEC-HMS model for prediction of future rainfall runoff in the Daecheong Dam basin of the Geum River."

Journal of Climate Change Research, KSCC, Vol. 11, No. 6-1, pp. 609-619.

Kousari, M.R., Malekinezhad, H., Ahani, H., and Asadi Zarch, M.A. (2010). "Sensitivity analysis and impact quantification of the main factors affecting peak discharge in the SCS curve number method: An analysis of Iranian watersheds." *Quaternary International*, Pergamon, Vol. 226, No. 1-2, pp. 66-74.

Kwak, J., Kim, J., Jun, S.M., Hwang, S., Lee, S., Lee, J.N., and Kang, M.S. (2020). "Assessment of future flood according to climate change, rainfall distribution and CN." *Journal of the Korean Society of Agricultural Engineers*, Vol. 62, No. 6, pp. 85-95.

Lee, J., and Shin, H. (2021). "Assessment of future climate change impact on an agricultural reservoir in South Korea." *Water*, MDPI AG, Vol. 13, No. 15, 2125.

Li, H.-C., Hsiao, Y.-H., Chang, C.-W., Chen, Y.-M., Lin, L.-Y., Chang, C.-W., Chen, Y.-M., Lin, L.-Y., and Michailidis, A. (2021). "Agriculture adaptation options for flood impacts under climate change - A simulation analysis in the Dajia River Basin." *Sustainability*, MDPI, Vol. 13, No. 13, 7311.

Ministry of Environmen (ME) (2019). *Standard guidelines for estimating flood*. Publication No. 11-148000- 001604-14 (in Korean).

Ministry of Land, Transport and Maritime Affairs (MLTM) (2012). *Design flood estimation methods*. (in Korean).

Moazzam, M.F.U., Rahman, G., Munawar, S., Farid, N., and Lee, B.G. (2022). "Spatiotemporal rainfall variability and drought assessment during past five decades in South Korea using SPI and SPEI." *Atmosphere*, MDPI, Vol. 13, No. 2, 292.

Mohammad, A.G. (1978). "Flood routing by the Muskingum method." *Journal of Hydrology*, Vol. 36, pp. 353-363.

Park, S., Sur, C., Kim, J., Choi, S., Lee, J., and Kim, T. (2021). "Projected drought risk assessment from water balance perspectives in a changing climate." *International Journal of Climatology*, Wiley, Vol. 41, No. 4, pp. 2765-2777.

Perdikaris, J., Gharabaghi, B., and Rudra, R. (2018). "Reference time of concentration estimation for ungauged catchments." *Earth Science Research*, CSCE, Vol. 7, No. 2, 58.

Qin, X.S., and Lu, Y. (2014). "Study of climate change impact on flood frequencies: A combined weather generator and hydrological modeling approach." *Journal of Hydrometeorology*, Vol. 15, No. 3, pp. 1205-1219.

Rentschler, J., and Salhab, M. (2020). *People in Harm's Way: Flood exposure and poverty in 189 countries*, The World Bank, Washington, DC.

Son, K.-H., Lee, B.-J., and Bae, D.-H. (2010). "Assessment on flood characteristics changes using Multi-GCMs climate scenario." *Journal of Korea Water Resources Association*, KWRA, Vol. 43, No. 9, pp. 789-799.

Song, Y.H., Chung, E., and Shahid, S. (2021). "Spatiotemporal differences and uncertainties in projections of precipitation and temperature in South Korea from CMIP6 and CMIP5 general circulation model." *International Journal of Climatology*,

Wiley, Vol. 41, No. 13, pp. 5899-5919.

Tegegne, G., Melesse, A.M., and Worqlul, A.W. (2020). "Development of multi-model ensemble approach for enhanced assessment of impacts of climate change on climate extremes." *Science of the Total Environment*, Elsevier B.V., Vol. 704, 135357.

Tramblay, Y., Bouvier, C., Martin, C., Didon-Lescot, J.-F., Todorovik, D., and Domergue, J.-M. (2010). "Assessment of initial soil moisture conditions for event-based rainfall-runoff modelling." *Journal of Hydrology*, Elsevier, Vol. 387, No. 3-4, pp. 176-187.

World Meteorological Organization (WMO) (2023). Atlas of mortality and economic losses from weather, climate and water-related hazards, accessed November 26 2023, <https://public-old.wmo.int/en/resources/atlas-of-mortality>.

Xu, C.-Y., Widénwid widén, E., and Halldin, S. (2005). "Modelling hydrological consequences of climate change-progress and challenges." *Advances in Atmospheric Sciences*, Vol. 22, No. 6, pp. 789-797.

Xu, K., Zhuang, Y., Bin, L., Wang, C., and Tian, F. (2023). "Impact assessment of climate change on compound flooding in a coastal city." *Journal of Hydrology*, Elsevier, Vol. 617, 129166.

Zhang, Y., Wang, Y., Chen, Y., Liang, F., and Liu, H. (2019). "Assessment of future flash flood inundations in coastal regions under climate change scenarios - A case study of Hadahe River basin in northeastern China." *Science of The Total Environment*, Elsevier, Vol. 693, 133550.